Applied Catalysis A: General 355 (2009) 169–175

Contents lists available at ScienceDirect

Applied Catalysis A: General

journal homepage: www.elsevier.com/locate/apcata

γ-MnO_2 octahedral molecular sieve: Preparation, characterization, and catalytic activity in the atmospheric oxidation of toluene

Lei Jin [a], Chun-hu Chen [a], Vincent Mark B. Crisostomo [a], Linping Xu [a], Young-Chan Son [a], Steven L. Suib [a,b,*]

[a] Department of Chemistry, University of Connecticut, U-3060, 55 North Eagleville Rd, Storrs, CT 06269-3060, USA
[b] Institute of Materials Science, University of Connecticut, U-3060, 55 North Eagleville Rd, Storrs, CT 06269-3060, USA

ARTICLE INFO

Article history:
Received 25 August 2008
Received in revised form 4 December 2008
Accepted 6 December 2008
Available online 13 December 2008

Keywords:
Toluene
OMS
Reflux
γ-MnO_2
Oxygen
Benzoic acid

ABSTRACT

A synthesized γ-MnO_2 octahedral molecular sieve was characterized and used to catalyze solvent-free atmospheric oxidation of toluene with molecular oxygen. The γ-MnO_2 showed excellent catalytic activity and good selectivity under the mild atmospheric reflux system at a low temperature (110 °C). Under optimized conditions, a 47.8% conversion of toluene, along with 57% selectivity of benzoic acid and 15% of benzaldehyde were obtained. The effects of reaction time, amount of catalyst and initiator, and the reusability of the catalyst were investigated.

1. Introduction

Catalyzed oxidation of aromatic hydrocarbons with molecular oxygen has been studied for several decades. For example, toluene can be converted into oxidation products such as benzyl alcohol, benzaldehyde, and benzoic acid. Liquid phase toluene oxidation with homogeneous metal salt catalysts has been realized industrially in the Rhodia, Dow, and Snia-Biscosa process using oxygen or peroxides as oxidants [1–4]. These processes operate at 165 °C and in 10 atm of air in the presence of a homogeneous cobalt catalyst in acetic acid. At present, the principal industrial production of benzoic acid via the oxidation of toluene involves the use of homogeneous cobalt catalysts in an air pressurized aqueous acetic acid mixture in the presence of Mn ions [5]. However, the use of solvent causes difficulties in the separation of catalysts and products, equipment corrosion, and due to the environmental hazards associated with the use of liquid acids as solvent. Developing solvent free toluene oxidation having great activity has attracted special attention as a promising environmentally friendly reaction.

Development of efficient heterogeneous catalysts has been devoted to a solvent free toluene oxidation system due to their convenient use and facile recycling [6–11]. For example, Wang et al. reported liquid phase toluene oxidation with molecular oxygen over copper-based metal oxides. In this process, however, in order to observe good conversion, a closed capacity autoclave, oxygen pressure, and higher temperature ($T > 160$ °C) were used. These common reaction conditions are too dangerous due to the explosion hazards of toluene-oxygen vapors at high reaction temperatures [12,13,22]. Thus, improvement of toluene oxidation with an atmospheric safe reflux system is a more acceptable pathway. But the comparatively low conversion at atmospheric pressure is another problem due to the challenge of oxidizing sp^3 hybridized carbon in inactive hydrocarbons [13–17] (Scheme 1).

Manganese oxide octahedral molecular sieves (OMS) have been applied extensively in energy storage, catalysis, battery electrodes, sensor materials, and ion sieves because of their distinctive properties [18–22]. γ-MnO_2 octahedral molecular sieve (also called chemical manganese dioxide, CMD), a disordered 1×1 and 1×2 tunnel structure corner shared with MnO_6 octahedral chains (Scheme 2), is one of these most useful manganese oxides and has been widely applied in the battery industry because of its high activity, low cost of raw material, and low toxicity. About 200,000 metric tons of γ-MnO_2 is used in the battery industry each year and significant effort has been expended to optimize and improve these materials [23,24]. Meanwhile, oxidation of aromatic

* Corresponding author at: Department of Chemistry, University of Connecticut, U-3060, 55 North Eagleville Rd, Storrs, CT 06269-3060, USA. Tel.: +1 860 486 2797; fax: +1 860 486 2981.
E-mail address: Steven.Suib@uconn.edu (S.L. Suib).

0926-860X/$ – see front matter © 2008 Elsevier B.V. All rights reserved.
doi:10.1016/j.apcata.2008.12.012

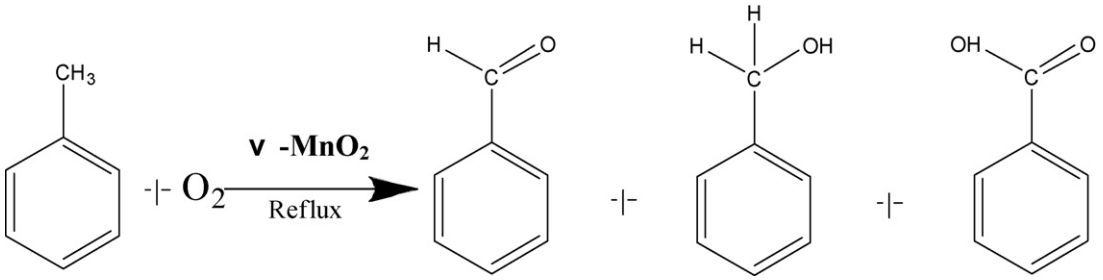

Scheme 1. Atmospheric oxidation of toluene with molecular oxygen using γ-MnO_2 catalyst.

hydrocarbons using γ-MnO_2 octahedral molecular sieve as the catalyst has not been reported.

In this work, we report the solvent free oxidation of toluene with molecular oxygen in an atmospheric reflux safe system using synthesized γ-MnO_2 octahedral molecular sieve as the catalyst. Significantly high conversion (47.8%) of toluene and good selectivity towards benzaldehyde (15%) and benzoic acid (57%) were obtained in an atmospheric system. To the best of our knowledge, this is the first example of γ-MnO_2 octahedral molecular sieve catalyzed active oxidation of toluene with molecular oxygen in a liquid phase reflux system.

2. Experimental

2.1. Preparation of γ-MnO_2 catalysts

The γ-MnO_2 catalyst was prepared by an *in situ* precipitation method. A known amount of potassium permanganate was dissolved in 100 mL distilled water. The solution was then added dropwise to a hot aqueous solution (90 °C, refluxing) containing 0.1 M of $MnSO_4$ and 6 mL of concentrated nitric acid under vigorous stirring. After refluxing the resulting solution for 24 h, the precipitate was filtered and washed with distilled water to remove by-products, followed by drying overnight at 100 °C.

2.2. Catalyst characterization

2.2.1. X-ray powder diffraction

The γ-MnO_2 catalyst was characterized by X-ray powder diffraction. The XRD patterns were obtained using a Scintag 2000 XDS instrument with a Cu Kα X-ray source with a beam voltage of 45 KV and 40 mA beam current.

2.2.2. Transmission electron microscopy

High-resolution transmission electron microscopy (HRTEM) was also used to check the morphology and structure of the catalyst. HRTEM studies were carried using a JEOL 2010 instrument with an accelerating voltage of 200 kV. The samples were prepared by dispersing the material in 2-propanol. Then a drop of the dispersion was placed on a carbon-coated copper grid and allowed to dry.

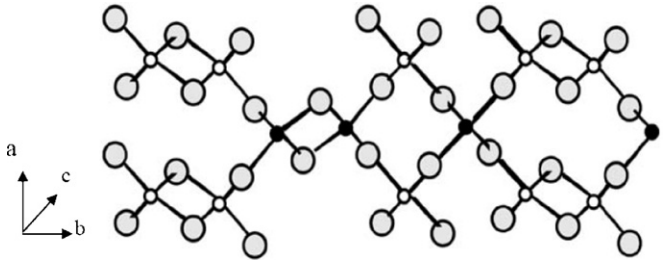

Scheme 2. Schematic structure of γ-MnO_2: views of a pyrolusite and ramsdellite intergrowth along *c*-axis. Open and filled small circles represent Mn atoms and open large circles represent O atoms respectively [27]. Reproduced with permission from Elsevier, Fig. 1e of Ref. [27].

2.2.3. Surface area

The surface area (SA) of γ-MnO_2 was measured using the Brunauer–Emmet–Teller (BET) method on a Micromeritics ASAP 2010 instrument. The area was determined to be 18 $m^2\ g^{-1}$ using N_2 as the adsorbent using the s multipoint method.

2.2.4. High-resolution scanning electron microscopy

HRSEM photographs were taken on a Zeiss DSM 982 Gemini emission scanning microscope with a Schottky Emitter at an accelerating voltage of 2 kV with a beam current of 1 μA. The samples were ultrasonically dispersed in ethanol for analysis. The suspensions were deposited on a gold-coated silicon wafer.

2.2.5. Catalytic reactions

All experiments were carried out in a three-necked round-bottom flask equipped with a condenser; a 9 mL/min of O_2 flow into the solution at atmospheric pressure, and the flask was placed in an oil bath at a temperature of 110 °C. In a typical reaction, toluene (10 mL, 0.094 mol) with 0.1 mol% of AIBN (2,2′-azobis(i-sobutyronitrile), a very commonly used radical initiator for the polymerization of vinyl monomers [34]) and 70 mg of catalyst (pretreated at 120 °C for 6 h) were introduced into the reactor. After refluxing for 20 h, the products were dissolved in acetonitrile and analyzed by an HP 5890 Series II gas chromatograph coupled with an HP 5971 mass detector. The column used was a nonpolar cross-linked siloxane (HP-1) with dimensions of 12.5 m × 0.2 m × 0.33 μm.

3. Results

3.1. X-ray powder diffraction (XRD)

The XRD pattern of the as-synthesized catalyst is shown in Fig. 1a, showing some broad peaks and some sharp peaks, as well as shifting. The broadening of diffraction peaks is known to occur for certain types of random intergrowths of ramsdellite (1 × 2 tunnel structure) and pyrolusite (1 × 2 tunnel structure) of manganese dioxide based on the "De Wolff model" published in 1959 [25]. Fig. 1c gives reference data for IBA-11 XRD patterns [26] of γ-MnO_2. As can be seen by comparing Fig. 1a and c, a pure crystalline gamma manganese dioxide was successfully synthesized.

3.2. SA and HRSEM

The surface area and pore volumes have also been tabulated in Table 1. The synthesized γ-MnO_2 did not have a high surface area (18 m^2/g) and total pore volume (0.0197 cm^3/g). The HRSEM picture (Fig. 2a) illustrated that the as-synthesized catalyst is made

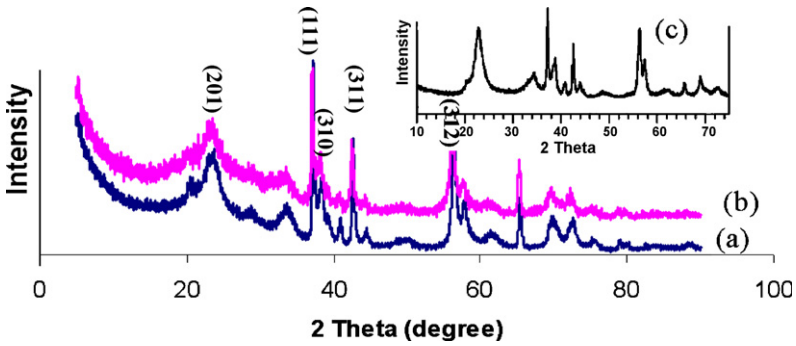

Fig. 1. X-Ray diffraction pattern of (a) as-synthesized fresh γ-MnO_2, (b) used γ-MnO_2, (c) pattern similar to that of IBA 11; Pr = 0.44, Tw = 26, Mt = 24 [27]. Reproduced with permission from Elsevier, Fig. 3b of Ref. [27].

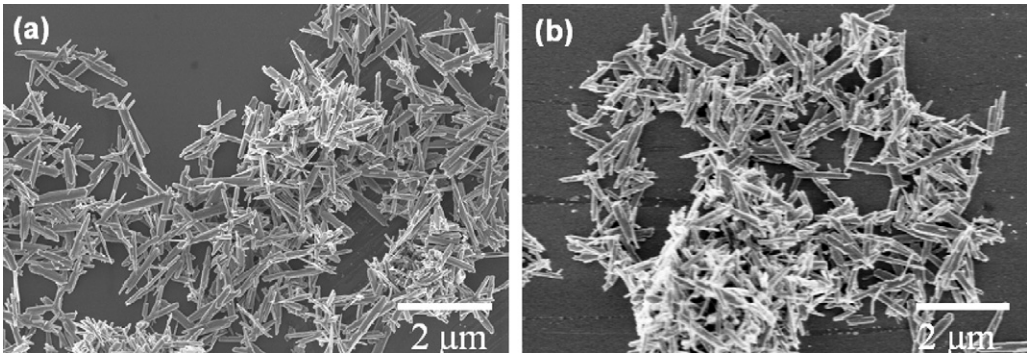

Fig. 2. Electron microscopy images of synthesized γ-MnO_2: (a) fresh γ-MnO_2 catalyst; (b) used γ-MnO_2 catalyst. Reproduced with permission from Elsevier, Fig. 3b of Ref. [27].

Table 1
Surface area and pore volumes of the synthesized catalyst and toluene oxidation catalysis.

BET SA (m^2/g)	Toluene conversion (%)					
	Total pore volume (cm^3/g)	Average pore diameter (Å)	20 h	TON[a]	48 h	TON
18	0.0197	19.3	17.6%	21	47.8%	56

Reaction conditions: 70 mg of the catalyst was mixed ultrasonically in 10 mL toluene and 0.1 mol% AIBN. Reflux at 110 °C for hours while bubbling O_2 with constant flow rate of 9 mL/min.
AIBN: 2,2′-azobis(isobutyronitrile).
[a] TON: Turn Over Number = mol of converted toluene/mol of catalysts used = (Conv. × 10 mL × 0.87 g mL^{-1}/92.4 g mol^{-1})/(0.07 g/87 g mol^{-1}).

up of homogeneous nanofibers that are around 1 μm in length and 50 nm in diameter.

3.3. HRTEM

The high-resolution transmission electron microscopy (HRTEM) image of a nanofiber (Fig. 3) shows lattice fringes, identified as (2 0 1) planes, based on d_{201} = 0.38 nm, which are parallel to the surface of the nanofibers. Likewise, the features observed in the TEM image show broken lattice fringes, which might correspond to structural defects and distortion of γ-MnO_2 as reported in the literature [25–31]. These defects and distortions are important for the catalytic activity of the γ-MnO_2 [27]. Results of selected area electron diffraction (SAED) illustrated in Fig. 3c shows striped-like spots, which could also be due to the intergrowth of the ramsdellite and pyrolusite structures.

3.4. Catalytic activity

Commercial MnO_2 and Mn_2O_3 gave no conversion. No conversion was observed for the blank run without a catalyst as well, as shown in Table 2. K-OMS-2 (cryptomelane phase 2 × 2 octahedral molecule sieve) based materials evaluated in Table 2 gave a very small (0.7%) conversion, even though these materials have been confirmed to be highly active in many catalytic reactions [32,33,35,37]. However, by using the synthesized γ-MnO_2, 17.6% conversion was achieved, indicating that the as-synthesized γ-MnO_2 is very active for toluene oxidation in our atmospheric and easily operated reaction system. Selectivities of 58% and 24% formed benzoic acid and benzaldehyde respectively were observed. Mass transfer limitations have been investigated by varying the stirring rate from 0 to 300 rpm. Very similar conversions as well as similar selectivities to benzaldehyde and benzoic acid were obtained, confirming that there are no mass transfer limitations under these particular conditions.

Table 2
Results of toluene oxidation by different catalysts.

Description	Surface area (m^2/g)	Selectivity (%)			Conv (%)
		Bzdh[c]	Bzal[d]	Bzad[e]	
Commercial MnO_2[b]	<2				0.0
Commercial Mn_2O_3[b]	<2	0	0	0	0.0
No catalyst	N/A[a]	0	0	0	0.0
K-OMS-2 [35]	65	100	0	0	0.7
Amorphous OMS [37]	257	0	0	0	0.0
H-K-OMS-2 [33]	62	0	0	0	0.0
Commercial CMD[b]	28	42	10	48	7.8
As-synthesized catalyst	18	24	7	58	17.6

Reaction conditions: 70 mg of catalysts was mixed ultrasonically in 10 mL toluene and 0.1 mol% AIBN. Reflux at 110 °C for 20 h while bubbling O_2 with constant flow rate of 9 mL/min.
[a] Not available.
[b] Chemicals purchased from Aldrich.
[c] Benzaldehyde.
[d] Benzyl alcohol.
[e] Benzoic acid.

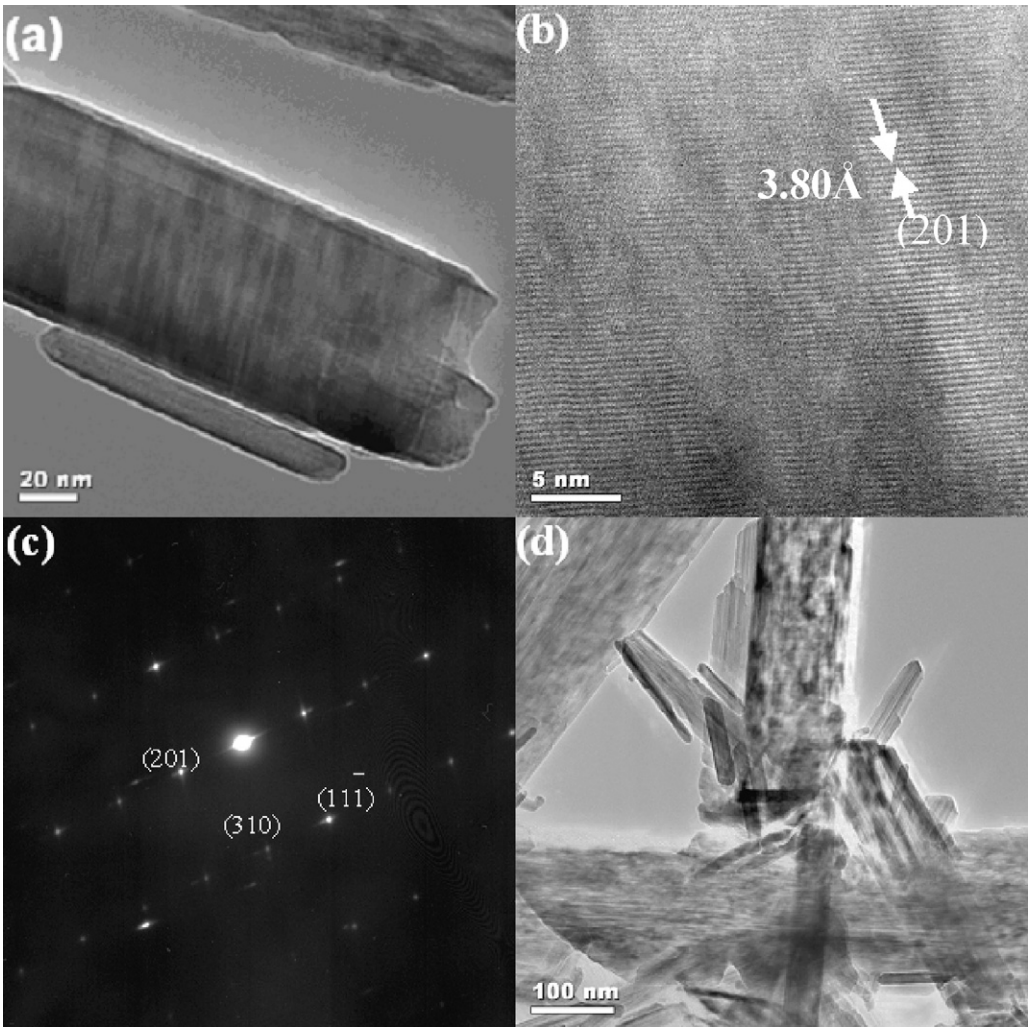

Fig. 3. HRTEM images of synthesized γ-MnO_2, showing lattice fringes of (2 0 1) planes (d = 3.80 Å).

4. Discussion

4.1. Synthesis and characterization

Highly active γ-MnO_2 was successfully prepared by a simple *in situ* precipitation method. In acidic media, a redox reaction between MnO_4^- and Mn^{2+} is expected to spontaneously produce MnO_2 based on Eqs. (1) and (2).

$$MnO_4^-(l) + 4H^+(l) + 3e == MnO_2(s) + 2H_2O \qquad E^o = 1.68\,V \tag{1}$$

$$MnO_2(s) + 4H^+(l) + 2e == Mn^{2+}(l) + 2H_2O \qquad E^o = 1.22\,V \tag{2}$$

In this process, $KMnO_4$ solution was designed to be added dropwise into a hot Mn^{2+} solution (85 °C) to provide excess Mn^{2+} during the reaction. A spontaneous redox reaction occurs between the reactants dissolved in water. Since γ-MnO_2 has point defects of Mn^{4+} cations replaced by Mn^{2+} cations [25], Mn^{4+}/Mn^{2+} replacement occurred immediately with energy provided by heating during the addition of MnO_4^-, and γ-MnO_2 was formed. K-OMS-2 was obtained instead of γ-MnO_2 when the heating step during the addition of $KMnO_4$ to Mn^{2+} solution is removed. In the conventional K-OMS-2 synthesis, the 2 × 2 tunnel structure is formed primarily due to two synergistic factors—heating and the presence of K^+ as the structure directing agent [35]. In our case, there is insufficient K^+ during the redox reaction (while $KMnO_4$ is being added to a heated Mn^{2+} solution), hence a different tunnel structure is obtained. Further theoretical and empirical research on the crystal structure of the synthesized γ-MnO_2 is still ongoing.

The crystal structure of the γ-MnO_2 was confirmed by XRD, TEM, and selected area electron diffraction (SAED). Peak broadening can be seen in the XRD pattern (Fig. 1). According to models of defects in γ-MnO_2 proposed by De Wolff [25], who described and discussed the effects in reciprocal space, γ-MnO_2 is a highly disordered material, and the broadening was proposed to be due to varying amounts of intergrowth of pyrolusite (1 × 1) and ramsdellite (1 × 2) phases. Comparing the XRD pattern Fig. 1a of the synthesized material and the reference commercial IBA-11 material (Fig. 1c), the γ-MnO_2 structure was confirmed. The spacing of the lattice fringes (3.8 Å) shown in Fig. 3b corresponds to the (2 0 1) plane, and many defects in the lattice can also be seen in the TEM image. Electron diffraction of γ-MnO_2 with typical intergrowth striped-like spots (Fig. 3c) provides further evidence for the distorted structure discussed above.

4.2. Catalytic reactions

To screen for factors that contribute to the conversion and selectivity of toluene oxidation, several kinds of the same family of

manganese oxide octahedral molecular sieves were tried as catalysts. Table 2 lists the conversions and selectivities of benzaldehyde, benzyl alcohol, and benzoic acid. Commercial Mn_2O_3 and MnO_2 (pyrolusite 1×1) as catalysts do not exhibit any catalytic activity for toluene oxidation, and only less than 0.7% conversion could be obtained when using highly catalytic active mixed-valence K-OMS-2 (cryptomelane 2×2) based materials. However, the as-synthesized γ-MnO_2 used in this work has a higher catalytic activity (17.6% conversion, along with 58% selectivity to benzoic acid and 24% selectivity to benzaldehyde as shown in Table 2) in this system, which is possibly due to the large amount of defects and distortion in the catalyst structure as discussed above. Commercial γ-MnO_2 (Aldrich activated MnO_2, crystal structure characterized by powder X-ray diffraction) has also been screened under the same conditions. A conversion of 7.8% was obtained. Surface areas of all the catalysts are also listed in Table 2, but no direct relationship between surface area and catalytic activity was found in this case. These observations may suggest that the γ-phase manganese oxide is the appropriate catalyst in the atmospheric toluene oxidation system and the as-synthesized γ-MnO_2 has better catalytic activity than selected commercial γ-MnO_2.

A reaction kinetic study of the toluene oxidation in this work was investigated by monitoring the catalytic oxidation of 10 mL of toluene at 110 °C in the presence of a constant feed of oxygen over a period of 48 h. The conversion of toluene increases continuously as time increases and 47.8% conversion of toluene was obtained after 48 h of reaction. A linear relationship ($r^2 = 0.98$) between conversion and time was obtained (Fig. 4). This indicates a zero order dependence on toluene concentration. Selectivity of products as a function of time is plotted in Fig. 5. Results of selectivity to benzaldehyde and benzoic acid suggest that the present refluxing process produces good selectivity of the products. Benzaldehyde was observed at the early stage of the reaction with selectivity higher than 90%. As the reaction proceeded, the selectivity to benzoic acid increased and remained at a high level (57–60%). A high yield can be obtained when the selectivity is steady as conversion increases. After 48 h of reaction, the selectivity does not vary a great deal as conversion increases. This suggests that the refluxing atmospheric conditions we report here represent a promising high-yield process.

The effect of amount of catalysts on the reaction was studied by varying the catalysts between zero and 140 mg; other reactions conditions remained the same. The results listed in Fig. 6 demonstrate clearly that as-synthesized γ-MnO_2 is very active in this reaction system, and that even small amounts (15 mg) can lead to significant conversion (12.1%). With the use of 35 mg of the catalyst, the conversion (16.8%) is almost invariant with respect to conditions of 70 mg of the catalyst (17.6%). This observation suggests that the conversion might be limited by the solubility of oxygen, which is constant under these reaction conditions [40].

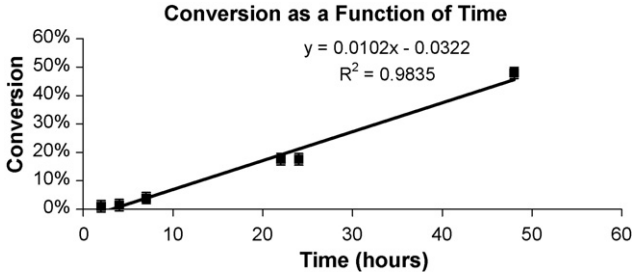

Fig. 4. The effect of time on conversion. *Reaction conditions*: 70 mg of the catalyst was mixed ultrasonically in 10 mL toluene and 0.1 mol% AIBN. Reflux at 110 °C for a period of time while bubbling O_2 with constant flow rate of 9 mL/min. AIBN: 2,2′-azobis(isobutyronitrile).

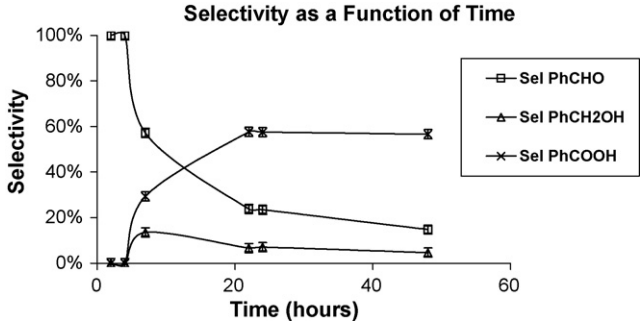

Fig. 5. The effect of time on selectivity. Reaction conditions are the same as those in Fig. 4.

However, with higher amounts of the catalyst the conversion of toluene decreases. Sheldon [36] observed that sometimes metal complexes of transition metals, especially in media of low polarity such as neat hydrocarbons, often act as catalysts at low loadings but as inhibitors at high loadings. High loadings of the catalyst may actually favor the homolytic decomposition of the AIBN. If more radicals are formed due to higher loadings of the catalyst, a higher percentage of the radicals could combine with each other to terminate the radicals. As a result less conversion of toluene took place, as can be seen in Fig. 6. Varying the amount of catalyst did not affect the selectivity of benzaldehyde (24–36%) and benzoic acid (48–58%) a great deal. An amount of 70 mg of the catalyst was chosen as the optimum amount in this particular atmospheric toluene oxidation system.

Results using various amounts of AIBN in our system are shown in Fig. 7. Higher amounts (0.4 mol%) of AIBN decrease the activity of the catalyst. This is due to termination of radicals that occurs on the surface of the catalyst. Due to these side reactions, the efficiency of radicals toward oxidation may be lower at higher concentrations of radicals than at lower concentrations. Likewise, lower amounts of AIBN (0.5 mol%) decrease the conversion of toluene due to the lack of radicals in the system. The optimum amount of AIBN for our toluene oxidation system is 0.1 mol% in toluene. The selectivity of products was not affected a great deal (56–60% to benzoic acid) by varying the amount of AIBN.

When the oxidation reaction of toluene with γ-MnO_2 was performed without any AIBN initiator, no toluene conversion was obtained. This result suggests, to a certain extent, a free radical autoxidation pathway. The oxidation reaction of toluene with AIBN in N_2 was also investigated, and no toluene conversion was observed either. These results suggest the possible oxidation pathways shown in Eqs. (3)–(11).

$$N{\equiv}C{-}CH_2{-}N{=}N{-}CH_2{-}C{\equiv}N \rightarrow 2N{\equiv}C{-}CH_2^{\bullet} + N_2 \quad (3)$$

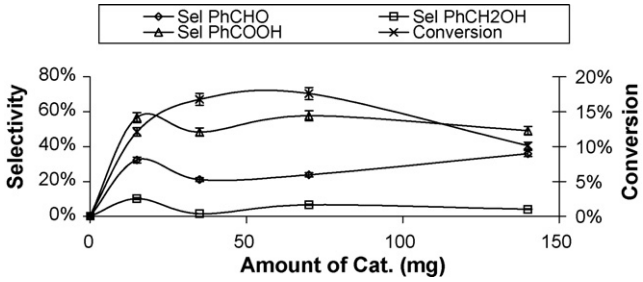

Fig. 6. The effects of amounts of catalysts on the conversions and selectivities. *Reaction conditions*: Different amounts of the catalyst were mixed ultrasonically in 10 mL toluene and 0.1 mol% AIBN. Reflux at 110 °C for 20 h while bubbling O_2 with constant flow rate of 9 mL/min.

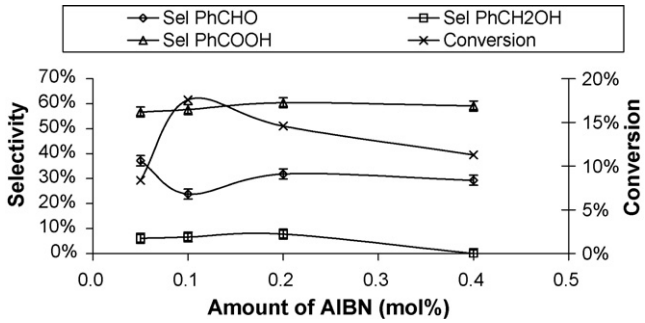

Fig. 7. The effects of amounts of AIBN on the conversions and selectivities. *Reaction conditions*: 70 mg of the catalyst was mixed ultrasonically in 10 mL toluene and different amounts of AIBN. Reflux at 110 °C for 20 h while bubbling O_2 with constant flow rate of 9 mL/min.

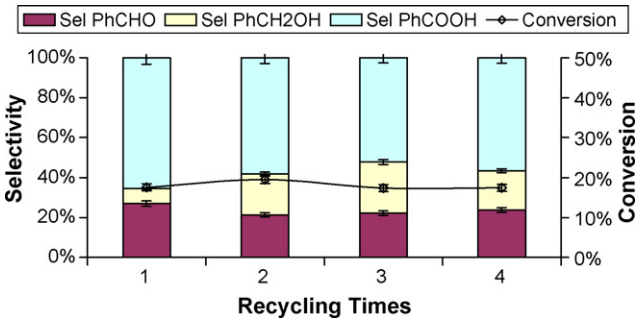

Fig. 8. Catalyst reusability tests. *Reaction conditions*: 70 mg of the catalyst was mixed ultrasonically in 10 mL toluene and 0.1 mol% AIBN. Reflux at 110 °C for 20 h while bubbling O_2 with constant flow rate of 9 mL/min.

$$PhCH_3 + N{\equiv}C{-}CH_2^{\bullet} \rightarrow PhCH_2^{\bullet} + N{\equiv}C{-}CH_3 \quad (4)$$

$$PhCH_2^{\bullet} + O_2 + Mn^{4+} \rightarrow PhCH_2OO^{\bullet} + Mn^{3+} \quad (5)$$

$$2PhCH_2OO^{\bullet} \rightarrow PhCHO + PhCH_2OH + O_2 \quad (6)$$

$$PhCH_2OO^{\bullet} + PhCH_3 \rightarrow PhCH_2OOH + PhCH_2^{\bullet} \quad (7)$$

$$PhCHO + PhCH_2OO^{\bullet} \rightarrow PhCH_2OOH + PhC^{\bullet}(O) \quad (8)$$

$$PhC^{\bullet}(O) + O_2 \rightarrow PhC(O)OO^{\bullet} \quad (9)$$

$$PhC(O)OO^{\bullet} + PhCH_3 \rightarrow PhCH_2^{\bullet} + PhC(O)OOH \quad (10)$$

$$PhC(O)OOH + 2Mn^{3+} + 2H^{+} \rightarrow PhC(O)OH + 2Mn^{4+} + H_2O \quad (11)$$

In which, AIBN helps to form the benzyl radical, which could form a peroxy radical via Mn(IV) in the γ-MnO_2 catalyst in the presence of O_2 (Eq. (5)). This peroxy radical can be decomposed to benzaldehyde and benzyl alcohol (Eq. (6)). The peroxy radical could also remove hydrogen from toluene or benzaldehyde as shown in Eqs. (7) and (8). The formed perbenzoic acid from Eq. (10) can be decomposed to benzoic acid by Mn(III) through an overall reaction as described in Eq. (11). Some other radicals are also involved in transfer reactions generating a stable product, for example, the reaction of bezyloxy radical (formed in the initiation reactions) removes hydrogen from toluene to form benzyl alcohol (Eq. (12)), and hydrogen abstraction from benzylhydroperoxide (formed in Eqs. (7) and (8)) and the benzylic position of benzyl alcohol under the influence of recycling of oxidation states [Mn(IV)/Mn(III)] in the γ-MnO_2 catalyst could also occur for benzaldehyde formation [38,39], Eqs. (13)–(18).

$$PhCH_2O^{\bullet} + PhCH_3 \rightarrow PhCH_2OH + PhCH_2^{\bullet} \quad (12)$$

$$PhCH_2OOH + Mn^{4} \rightarrow PhCH_2OO^{\bullet} + Mn^{3+} + H^{+} \quad (13)$$

$$PhCH_2OO^{\bullet} + Mn^{3+} \rightarrow PhCHO + Mn^{4+} + OH^{-} \quad (14)$$

$$PhCH_2OH + Mn^{4+} \rightarrow PhC^{\bullet}HOH + Mn^{3+} + H^{+} \quad (15)$$

$$PhC^{\bullet}HOH + O_2 \rightarrow PhCH(OH)OO^{\bullet} \quad (16)$$

$$PhCH(OH)OO^{\bullet} + Mn^{3+} + H^{+} \rightarrow PhCH(OH)OOH + Mn^{4+} \quad (17)$$

$$PhCH(OH)OOH \rightarrow PhCHO + H_2O_2 \quad (18)$$

Reusability tests of the synthesized γ-MnO_2 catalyst were also conducted in this work to investigate whether the catalyst could be recycled. After the reaction, the catalyst was filtered and washed with acetone and alcohol several times and dried at 120 °C overnight. The catalyst was then calcined at 200 °C to remove the alcohol and then used for another reaction. Fig. 8 shows the conversion and selectivity from the recycling experiments. The conversion of toluene and selectivity of benzoic acid and benzaldehyde are still maintained with respect to their original values. The XRD patterns (Fig. 1b) and HRSEM images (Fig. 2b) of the used catalysts indicate that the main characteristics of the catalyst were preserved during recycling.

5. Conclusion

Toluene atmospheric oxidation with molecular oxygen using a synthesized γ-MnO_2 octahedral molecular sieve catalyst resulted in promising conversions and selectivities in this atmospheric reflux safe system. Under optimum conditions, a 47.8% conversion of toluene, along with 57% selectivity of benzoic acid and 15% of benzaldehyde were obtained. The MnO_2 octahedral molecular sieve catalyst has promising reusability and can be recycled. A free radical reaction mechanism was also proposed in this work. Such an impressive activity and selectivity opens up new possibilities for activating aromatic hydrocarbons to synthesize the corresponding aldehydes and acids with molecular oxygen in the liquid phase atmospheric system. Further studies on the use of other substrates, reaction mechanism, and crystal structure of the catalyst are still ongoing.

Acknowledgements

We acknowledge support of the Chemical Sciences, Geosciences and Biosciences Division, Office of Basic Energy Sciences, Office of Science, US Department of Energy. We would also like to thank Dr. Francis Galasso, Dr. Raymond Joesten and Shanthakumar Sithambaram for many helpful discussions.

References

[1] Y. Ishii, S. Sakaguchi, T. Iwahama, Adv. Synth. Catal. 343 (2001) 393–427.
[2] K. Nomiya, K. Hashino, Y. Nemoto, M. Watanabe, J. Mol. Catal. A 176 (2001) 79–86.
[3] T. Garrell, S. Cohen, G.C. Dismukes, J. Mol. Catal. A 187 (2002) 3–15.
[4] Snia-Viscosa, Hydrocarbon Proc. 134 (1977) 210.
[5] H. Holtz, L. Garder, Phillips Petroleum Co., US Patent 4,088,823, 1978.
[6] M.A. Fox, M.T. Dulay, Chem. Rev. 93 (1993) 341;
(b) S.M. George, Chem. Rev. 95 (1995) 475–476.
[7] X. Li, J. Xu, F. Wang, J. Gao, L. Zhou, G. Yang, Catal. Lett. 108 (2006) 137–140.
[8] G. Huang, A.P. Wang, Y. Liu, Y.A. Guo, H. Zhou, S.K. Zhao, Catal. Lett. 114 (2007) 174–177.
[9] W.B. Li, W.B. Chu, M. Zhuang, J. Hua, Catal. Today 93–95 (2004) 205–209.
[10] X. Li, J. Xu, L. Zhou, F. Wang, J. Gao, C. Chen, J. Ning, H. Ma, Catal. Lett. 110 (2006) 255–260.
[11] F. Wang, J. Xu, X.Q. Li, J. Gao, L.P. Zhou, R. Ohnishi, Adv. Synth. Catal. 347 (2005) 1987–1992.
[12] M. Goethals, et al. J. Hazard. Mater. A 70 (1999) 93–104.

[13] R.A. Sheldon, H. Van Bekkum, Fine Chemicals through Heterogeneous Catalysis, Wiley–VCH, Weinheim, 2001, pp. 1–10.
[14] J.M. Thomas, R. Raja, G. Sankar, R.G. Bell, Nature 398 (1999) 227–230.
[15] S.S. Stahl, Angew. Chem. Int. Ed. 43 (2004) 3400–3420.
[16] C. Limberg, Angew. Chem. Int. Ed. 42 (2003) 5932–5954.
[17] A.D. Sadow, T.D. Tilley, Angew. Chem. Int. Ed. 42 (2003) 803–805.
[18] Y.F. Shen, P.R. Zerger, R.N. DeGuzman, S.L. Suib, L. McCurdy, D.I. Potter, C.L. O'Young, Science 260 (1993) 511–516.
[19] (a) O. Giraldo, S.L. Brock, W.S. Willis, M. Marquez, S.L. Suib, S. Ching, J. Am. Chem. Soc 122 (2000) 9330–9331;
(b) A.R. Armstrong, P.G. Bruce, Nature 381 (1996) 499–500.
[20] R. Ma, Y. Bando, L. Zhang, T. Sasaki, Adv. Mater 16 (2004) 918–922.
[21] Z.R. Tian, W. Tong, J.Y. Wang, N.G. Duan, V.V. Krishnan, S.L. Suib, Science 276 (1997) 926–927.
[22] Z.R. Tian, Y.G. Yin, S.L. Suib, C.L. O'Young, Chem. Mater. 9 (1997) 1126–1133.
[23] O. Schilling, J.R. Dahn, J. Appl. Cryst. 31 (1998) 396–406.
[24] D. Glover, B. Schumm, A. Kazowa, Handbook of Manganese Dioxides Battery Grade, Int. Battery Mater. Assoc., 1989.
[25] P.M. De Wolff, Acta Cryst. 12 (1959) 341.
[26] D.G. Malpas, F.L. Tye, in: D. Glover, B. Schumm, Jr., A. Kosawa (Eds.), Handbook of Manganese Dioxides Battery Grade, IBA Inc. & JEC Press Inc., Brunswick, 1989 (Chapter V).
[27] L.I. Hill, A. Verbaere, J. Solid. State Chem. 177 (2004) 4706–4721.
[28] E. Levi, E. Zinigrad, H. Teler, M.D. Levi, D. Aurbach, J. Electrochem. Soc. 145 (October (10)) (1998).
[29] R. Strobel, J.-C. Joubert, J. Mater. Sci. 21 (1986) 583.
[30] L.A.H. MacLean, F.L. Tye, J. Solid State Chem. 123 (1996) 150–160.
[31] A. Le Gal La Salle, S. Sarciaux, A. Verbaere, Y. Piffard, D. Guyomard, J. Electrochem. Soc. 147 (2000) 945–952.
[32] J.-Y. Wang, G.-G. Xia, Y.-G. Yin, S.L. Suib, C.L. O'Young, J. Catal. 176 (1998) 275–284.
[33] Y.C. Son, V.D. Makwana, A. Howell, S.L. Suib, Angew. Chem. Int. Ed. 40 (22) (2001) 4280–4283.
[34] G. Xu, R.R. Nambiar, F.D. Blum, J. Colloid Interface Sci. 302 (2006) 658–661.
[35] R.N. De Guzman, Y.F. Shen, E.J. Neth, S.L. Suib, C.L. O'Young, S. Levine, J.M. Newsam, Chem. Mater. 6 (1994) 815–821.
[36] R.A. Sheldon, Metal-Catalyzed Oxidation of Organic Compounds, Academic Press, New York, 1981.
[37] S.R. Segal, S.L. Suib, Chem. Mater. 11 (1999) 1687–1695.
[38] V.D. Makwana, Y.C. Son, A.R. Howell, S.L. Suib, J. Catal. 210 (2002) 46–52.
[39] J.A.A. Horn, P.L. Alsters, G.F. Versteeg, Int. J. Chem. React. Eng. 3 (2005) A6.
[40] A.R. Li, S.W. Tang, P.H. Tan, C.J. Liu, B. Liang, J. Chem. Eng. Data 52 (2007) 2339–2344.